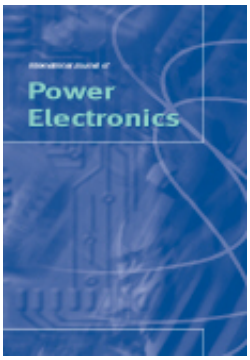

International Journal of Power Electronics

ISSN online: 1756-6398 - ISSN print: 1756-638X
https://www.inderscience.com/ijpelec

An alternate topology for multi-input DC-DC converter with performance analysis

Tuhinanshu Mishra, Ravindra Kumar Singh

DOI: 10.1504/IJPELEC.2025.10068271

Article History:

Received:	13 May 2024
Last revised:	17 August 2024
Accepted:	31 August 2024
Published online:	15 January 2025

An alternate topology for multi-input DC-DC converter with performance analysis

Tuhinanshu Mishra* and
Ravindra Kumar Singh

Department of Electrical Engineering,
Motilal Nehru National Institute of Technology,
Allahabad (Prayagraj), U.P., India
Email: tuhinanshu.2020ree07@mnnit.ac.in
Email: rksingh@mnnit.ac.in
*Corresponding author

Abstract: A single inductor dual-input single-output (DISO) DC-DC converter topology is presented in this paper. The proposed DISO topology utilises a 1-mH inductor and four switches. A 3-pulse novel PWM scheme and control strategy are introduced for efficient control. A PV source and a 36-V battery energy storage system are two sources. The 6-KW DC microgrid load consists of residential loads and electric vehicle charging station. With dropping solar irradiance, it is shown that the load demand is met by vehicle to grid transfer of power. Simulation against variation in solar irradiance from 0 W/m^2 to 1,000 W/m^2 in PV source is also done using MATLAB SIMULINK. The proposed converters performance under simulation in real time is done by using Novacor RTDS simulator along with its hardware prototype building. The converter together with the microgrid application is a rapidly emerging area of application of electronics in power system.

Keywords: multi-input multi-output; MIMO; renewable energy; microgrid; solar energy; EV charging.

Reference to this paper should be made as follows: Mishra, T. and Singh, R.K. (2025) 'An alternate topology for multi-input DC-DC converter with performance analysis', *Int. J. Power Electronics*, Vol. 21, No. 1, pp.69–95.

Biographical notes: Tuhinanshu Mishra pursued his BTech from the B.B.D.N.I.T.M. Lucknow and MTech from the U.C.E.R. Prayagraj. He is currently pursuing his PhD with Motilal Nehru National Institute of Technology Allahabad, Prayagraj, India. His area of specialisation is power electronic converter topologies, focusing on muti input multi-output converters.

Ravindra Kumar Singh received his BSc in Electrical Engineering from the Bhagalpur College of Engineering, Bhagalpur University, Bihar, India; Master of Technology in Power Electronics from Institute of Technology Banaras Hindu University (now IIT-BHU), India; and Doctorate from the Indian Institute of Technology Kanpur, Uttar Pradesh, India. He is currently a Professor in Electrical Engineering Department as well as the Dean Academics at Motilal Nehru National Institute of Technology Allahabad,

Prayagraj, India. His research interests include power electronics, DC-DC converters, modelling design and control of multiphase inverters – topology, modulation and control, PWM rectifiers, electrical machines and drives, power system protection and planning, energy storage, EV charging, systems, and control theory.

1 Introduction

Multiple sources in a converter are more reliable than a single source dependent converter power supply. Multiple-input multiple-output (MIMO) converters in comparison to parallel combination of sources (Chen et al., 2021) have smaller converter size, lesser losses and higher reliability. This has been is illustrated in Figure 1; wherein Figure 1(b), the number of conversion stages are lesser (MIMO) compared to Figure 1(a).

The proposed dual-input single-output (DISO) converter topology is a four switch and one inductor architecture with minimum losses and converter volume. The distinctive pulse-width modulation (PWM) signals initiate one source at a time removing cross coupling and facilitating independent load sharing along with having the capability of operating the DISO converter with either one or both sources simultaneously. The DISO operation is feasible in both buck and boost modes depending on the PWM and duty cycles of the switches.

The DISO configuration is fed by a hybrid combination of solar energy and battery energy storage systems (BESS) thus making it entirely independent of grid supply (Kim et al., 2021; Bussa et al., 2021). Power sharing between the dual sources is controlled by the PWM pulses. In case of unavailability of one of the sources, the PWM can be modified to feed the load by a single source thus controlling the intermittency of renewable power supply (Suresh et al., 2021).

Figure 2 shows the power flow from the combination of sources towards the DC microgrid and EV charging facility.

A DC microgrid can be naturally interfaced with renewable energy sources like PV panels and fuel cells along with modern day electronic devices (Pires et al., 2022, 2023; Sobral et al., 2023; Tian et al., 2023). The 6-KW DC microgrid assumed here as a load to the DISO converter application has four residential loads of 1 KW each in a rural microgrid and one EV charging station of 2 KW. The EV charging facility is made bidirectional capable of maintaining constant power at the DC bus in case of minimum solar irradiances and low state of charge (SOC) of the battery energy storage system (BESS) by vehicle to grid (V2G) transfer.

This article addresses all the issues occurring in such integration with the following contributions:

1 proposes a DISO converter topology, novel PWM scheme and calculation of parameters for converter design and implementation

2 provides a solution for maintaining load stability and performance in possible cases of irradiance drop to PV.

Figure 1 (a) Multiple inputs and multiple outputs realised by multiple DC-DC converters (b) Multiple inputs and multiple outputs realised by a MIMO converter (see online version for colours)

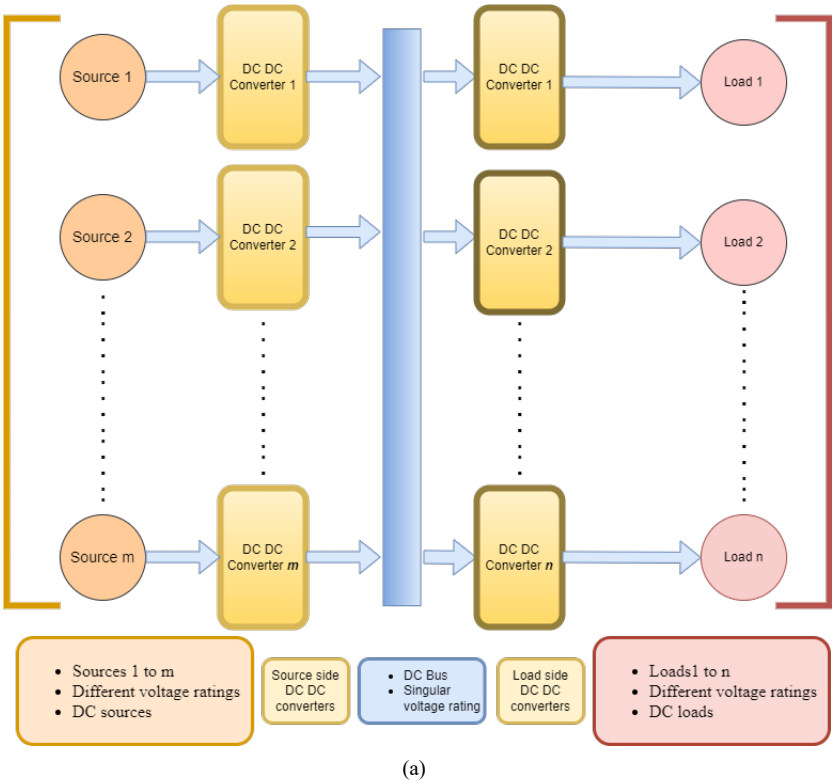

(a)

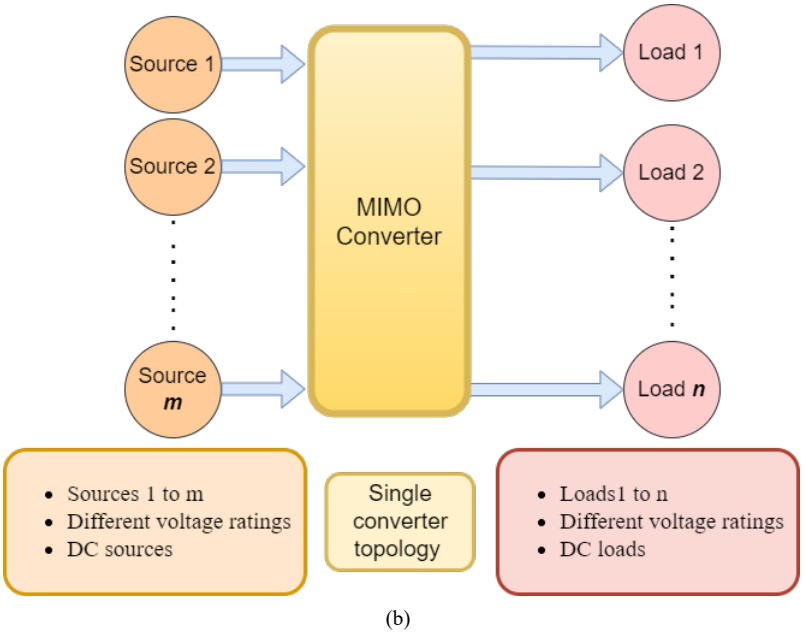

(b)

The rest of the article is organised as follows: Section 2 describes the proposed converter topology and discussions regarding topology. Section 3 is devoted to modes of operation with mathematical modelling. Section 4 describes the simulation results. Section 5 deals in control strategy for converter whereas Section 6 is devoted to hardware results and validation. Section 7 of the article deals in discussions about stability analysis and other performance parameters. The article is concluded in Section 8.

Figure 2 Power flow diagram (see online version for colours)

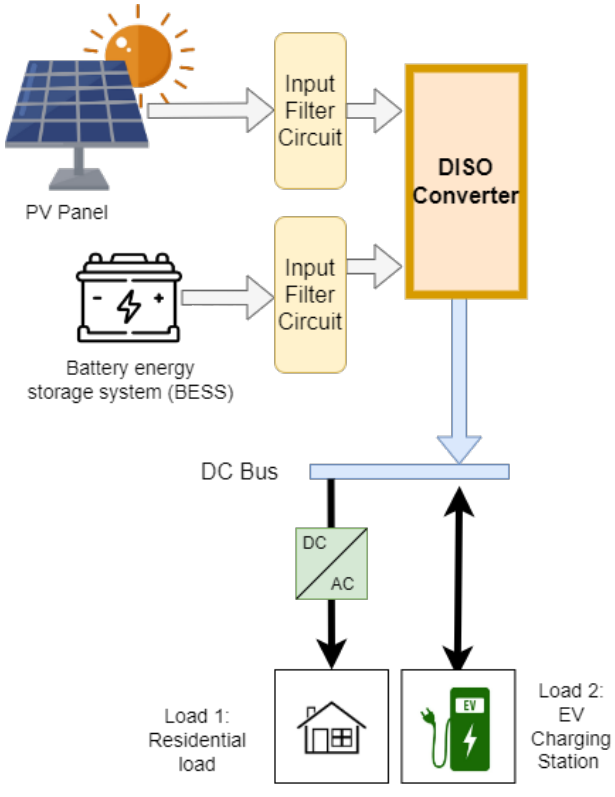

2 Converter operation

2.1 Proposed configuration

The proposed DISO configuration is shown in Figure 3. The four-switch structure offers advantage in terms of simplicity in operation as there is only a single inductor present. Since the number of inductors directly affect the size and overall system cost, the proposed DISO converter offers compact packaging and reduced cost. There are three diodes which ensure unidirectional operation of the converter in each mode. MOSFET switches are used since high switching frequency is desirable for ripple reduction and faster converter response is required when integrated with microgrid and EV chargers. Two voltage sources at the input port 1 and 2 are supplying power to the single output port loaded with an impedance.

Table 1 Comparison of proposed DISO topology with other existing topologies

Configuration							
Attributes	*Salimi et al.*	*Akar et al.*	*Dhananjay and Patnaik*	*Malik et al.*	*Athikkal et al.*	*Traditional DISO*	*Proposed DISO*
High frequency transformer	No	No	No	No	No	No	No
Conducting components in 1 cycle	6	9	6	10	5	6	3
Number of magnetics	2	2	2	n (outputs)	1	2	1
Diodes	2	2	No	3n	No	2	3
Intermediate capacitors	No	No	Yes, 1	Yes, 3n	No	No	No
DC link capacitors	1	1	1	1	1	1	1
Number of switches	6	4	5	1	4	2	4
Voltage ripple	Average	Low	Low	Average	Low	Average	Low
Current ripple	Average	Low	Low	Average	Low	Average	Low
Output voltage type (−ve or +ve)	+ve	+ve	+ve	+ve	+ve	+ve	+ve

Figure 3 Proposed single inductor dual input single output (DISO) converter circuit diagram (see online version for colours)

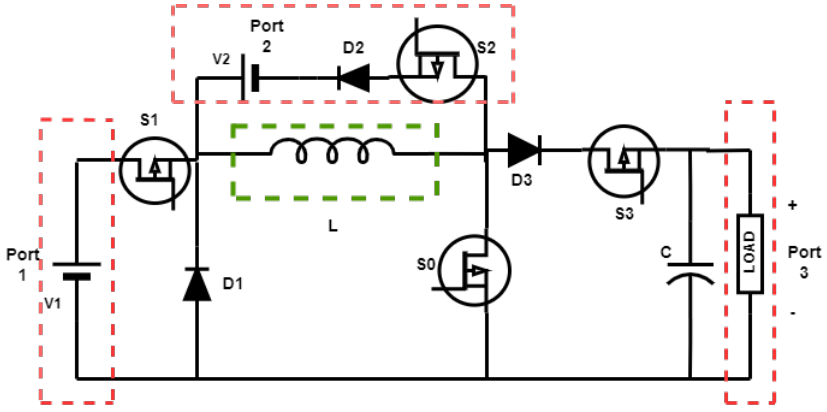

2.2 Comparative analysis

The existing literature reports several multi-input topologies in the recent developments in power converters. Salimi et al. (2021) developed DISO topology of DC-DC converter. However, the proposed converter can be compared to a pair of boost converters connected in parallel. Moreover, it is incapable of performing as a buck converter in appropriate modes. The proposed DISO topology in this paper is a novel topology not being cascade or parallel of two topologies. Also, it is capable of operating both as buck and boost converter. Akar et al. (2016) suggested a bidirectional non-isolated converter. Although the converter is highly efficient (more than 93%), it suffered from a major drawback. The increased number of ports led to increase in number of inductors. In the proposed topology increasing as many ports is possible without increasing the inductor. There shall be only one inductor in all cases. Another three port topology derived in Dhananjaya and Pattnaik (2020) consists of one input and two output ports. The proposed topology works in both buck and boost modes and the cross regulation problem has been eliminated, however use of multiple inductors and too many switches makes circuit inefficient when sizing and cost are considered. Malik et al. (2021) proposed a single-input multi-output converter. The paper has an interesting contribution that the entire topology is based on a single switch. However the number of inductors increases as we increase the number of outputs in the topology. Moreover, there is no provision of maintaining different voltage levels at different ports. All output voltages are compulsorily boosted. In proposed DISO, the two inputs can be at same or different voltage levels and still the desired output can be recorded. In case ports are increased, even then the voltage levels can be maintained different at each port.

A single inductor topology is proposed in Athikkal et al. (2019) which is capable of operating in both and buck and boost modes. The converter however, has a demerit that the operation is dependent on three different duty cycles thus making the closed loop operation and control extremely difficult. Furthermore, the converter operates in six modes that makes the converter operation complex. Proposed converter has only three modes of operation. Table 1 shows the comparison of various topologies on the basis of component count and other parameters.

2.3 Converter advantages

The proposed DISO converter topology in this article suffers from no such demerits and has the following advantages:

1 a single inductor is used in the topology amounting to compact size, lower cost, lesser power loss due to internal resistance in the coil

2 the converter has lesser components as compared to other DISO topologies which leads to and reduced weight and packaging volume

3 the converter is capable of both buck and boost modes of operations with varying duty cycles irrespective of the voltage level of the inputs

4 closed loop operation of the converter achieves desired voltage level at the output irrespective of the voltage level of the inputs

5 the load bus voltage can be maintained constant even if either one of the DC sources are absent

6 a novel PWM scheme suggested in the article simplifies control of the DISO topology.

3 Modes of operation

3.1 Mode 1: inductor charging by source 1

The inductor L is charged by source V1 through switches S0 and S1. Rest of the switches in the DISO topology are open. The inductor charging takes place unidirectionally from the source.

$$V_1 + L\frac{di}{dt} = 0 \tag{1}$$

The duty cycle D_1 of the two switches S_1 and S_0 is common since they are closed and opened simultaneously. Figure 5 shows the time duration of the gate pulses provided to the switches.

$$T = T_1on + T_2on + T_3on \tag{2}$$

Duty cycle D_1 can be expressed as:

$$D_1 = \left(\frac{T_{1on}}{T_{1on} + T_{2on} + T_{3on}}\right) \tag{3}$$

where T_1on is the time duration for which switches S_1 and S_0 are turned on simultaneously, T_2on is the time duration for which switch S_2 is turned on and T_3on is the time duration for which the switch S_3 is turned on.

Figure 4 Modes of operation of the proposed DISO in (a) mode 1: charging by source 1, (b) mode 2: charging by source 2 and (c) mode 3: discharging (see online version for colours)

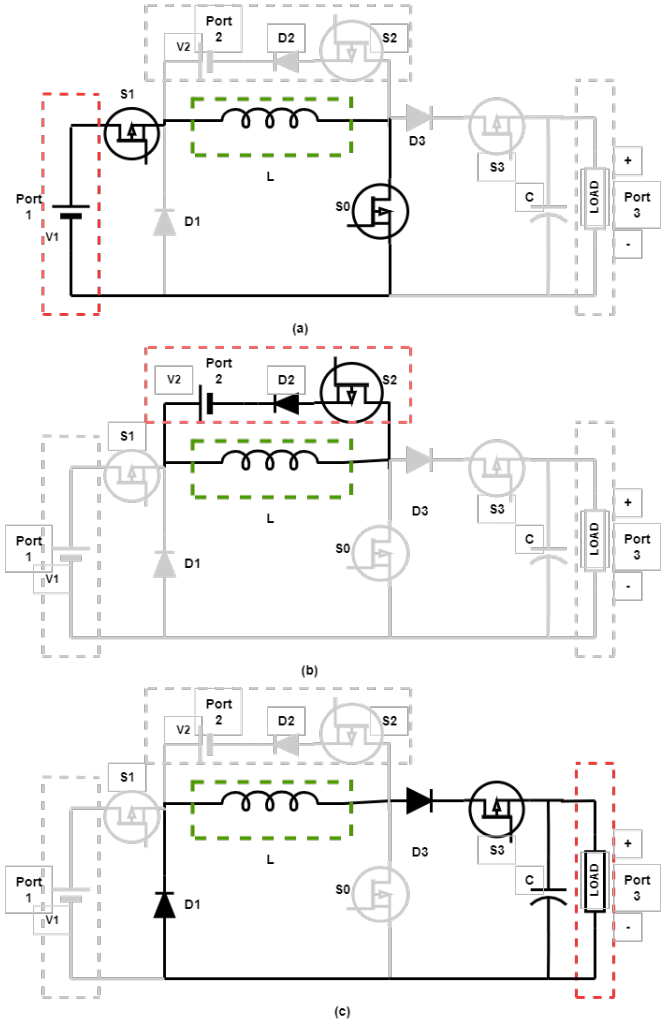

3.2 Mode 2: inductor charging by source 2

In this mode of operation, the inductor L is charged unidirectionally by the source V_2 through the switch S_2 and diode D_2. The condition of uninterrupted charging in this mode is that $V_2 \geq V_1$ else voltage across inductor will be greater than the voltage across the source and discharging will takes place in practicality in the form of heat loss.

$$V_2 + L\frac{di}{dt} = 0 \tag{4}$$

Duty cycle (D_2):

$$D_2 = \left(\frac{T_{2on}}{T_{1on} + T_{2on} + T_{3on}}\right) \tag{5}$$

3.3 Mode 3: inductor discharging through load

In the third mode of operation, the inductor acts as a source and discharges itself through the load at the output port. The power flow occurs from the inductor to the load through switch S_3, diodes D_1 and D_3. The capacitor acts as a voltage ripple filter for the output.

$$L\left(\frac{di}{dt}\right) - iR = 0$$

$$\frac{1}{i}\left(\frac{di}{dt}\right) = \frac{R}{L} \tag{6}$$

Duty cycle (D_3):

$$D_3 = \left(\frac{T_{3on}}{T_{1on} + T_{2on} + T_{3on}}\right) \tag{7}$$

The time period of each switch is independent of the time period of the other, the condition being that a switch is turned on only when the switch in present loop is turned off. No two independent loop switches can be turned on simultaneously. Switch S_0 and S_1 belong to the same charging loop hence turned on together. Switch S_2 and S_3 are of separate charging/discharging loops hence allotted separate time intervals. Thus, the converter operates in three different modes of operation with a unique PWM scheme. The switching sequence is depicted in Figure 5.

Figure 5 Switching sequence (see online version for colours)

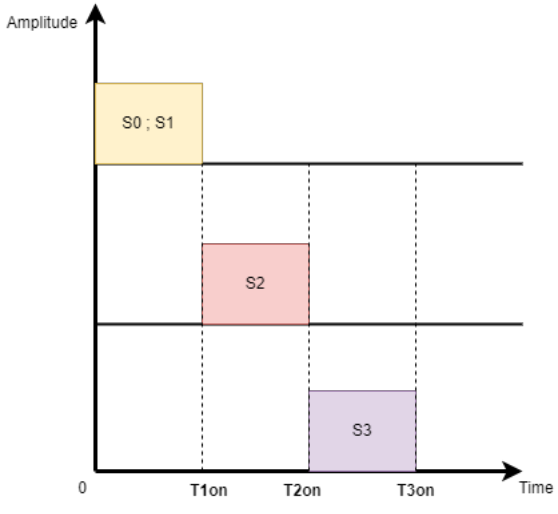

4 Simulation results and discussion

Solar irradiance is varied from 1,000 W/m^2 to 0 W/m^2 and it is observed that when the irradiance level drops down below the threshold value, then reverse transmission of power from vehicle to grid (V2G mode) takes place and the load voltage and load power can be constant.

Figure 6 (a) PV source voltage and (b) battery source voltage, current at 1,000 W/m^2 irradiance (see online version for colours)

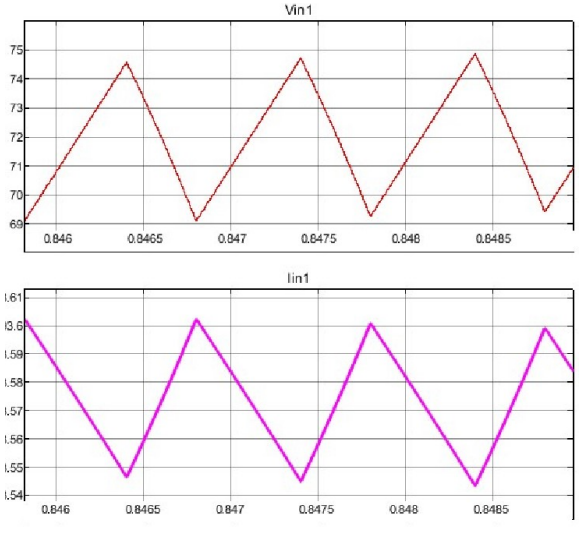

(a)

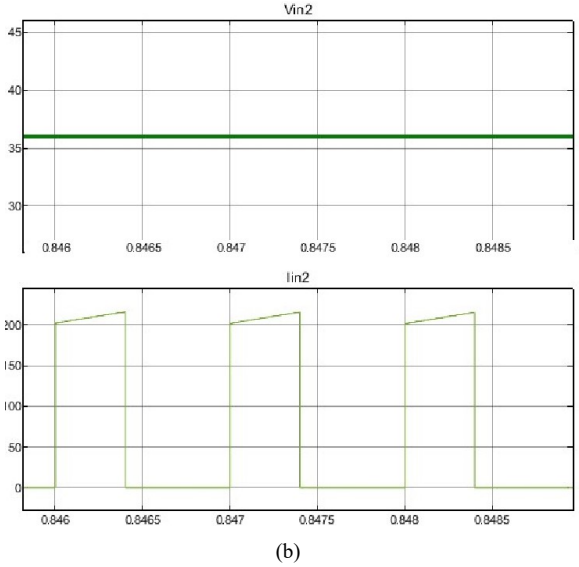

(b)

Figure 7 (a) PV source current and (b) battery current with 700 W/m^2 irradiance (see online version for colours)

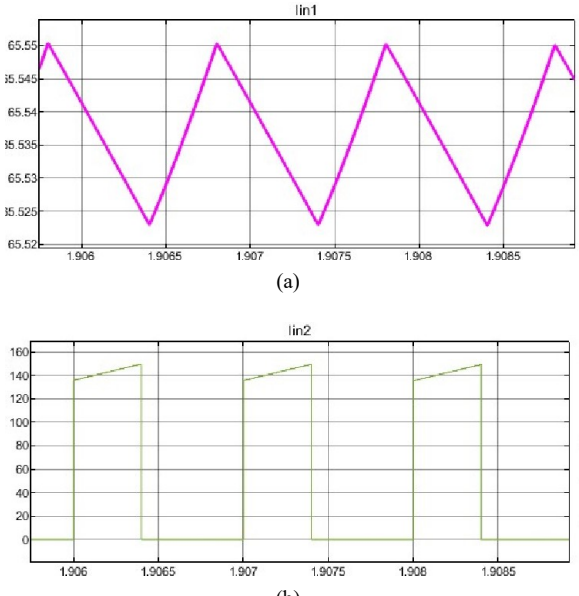

Figure 8 (a) PV source current and (b) battery current with 500 W/m^2 irradiance (see online version for colours)

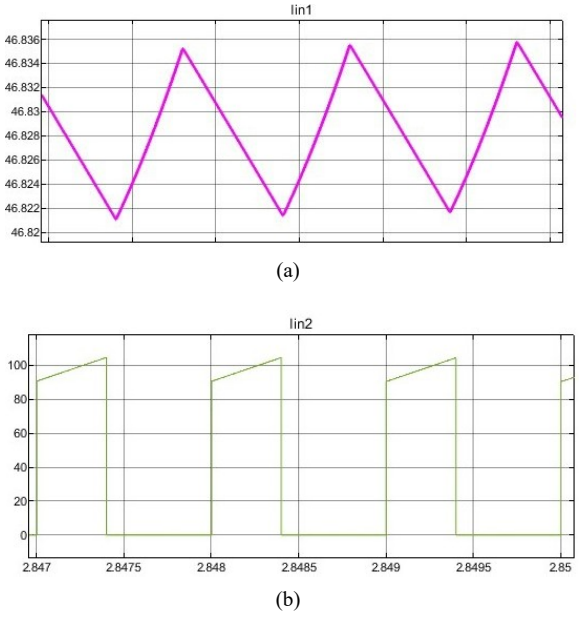

Figure 9 Battery current with 0 W/m^2 irradiance (see online version for colours)

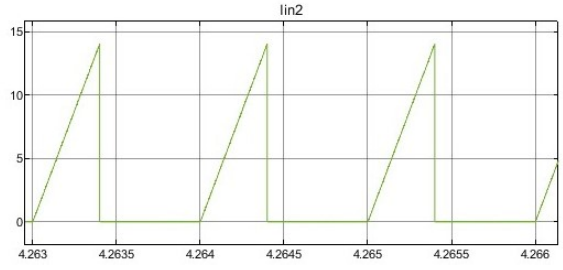

Figure 10 Inductor voltage and current (see online version for colours)

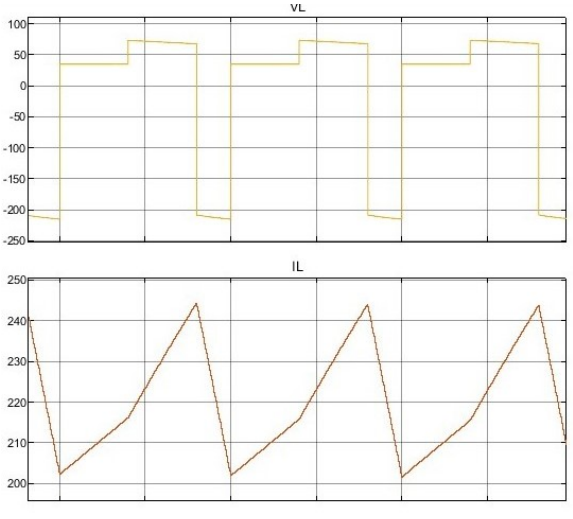

Figure 11 Average output voltages and currents at varying irradiances (see online version for colours)

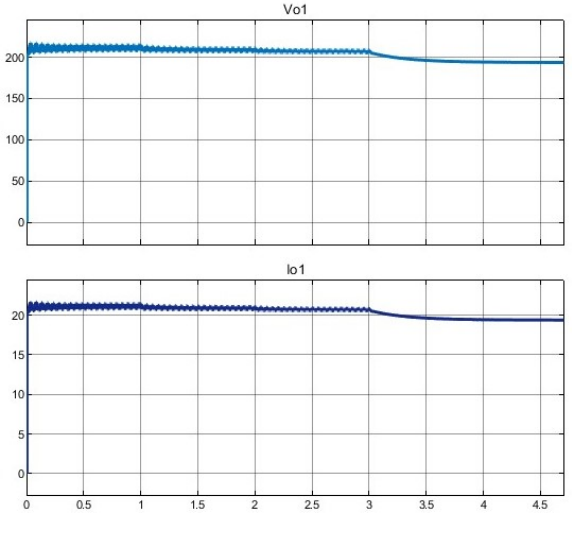

4.1 Supply voltages and currents

Voltage sources V_{in1} and V_{in1} are PV and battery sources, respectively. When the PV source is supplying power at full potential from maximum irradiance of $1{,}000$ W/m^2 then the supplied average voltage is 72 V and equivalent current of 68.5 A. Similarly 36 V is provided by the battery bank with an average current of 100 A. Figures 6–9 show the variation of supply power with varying irradiances. As the irradiance decreases to 0 W/m^2, the PV source current and battery currents decrease, however the source voltages are maintained constant.

At low irradiances, the load power demand exceeds the supply so the PID control strategy designed for the converter and enables reverse flow of power from vehicle charging station to the microgrid to maintain power stability. This mode is called the vehicle to grid mode (V2G) of power transmission. In this mode, the power that was earlier supplied for vehicle charging is utilised to maintain power equilibrium and voltage stabilisation at the load end.

Figure 12 Output voltages and currents at irradiance of (a) $1,000$ W/m^2, (b) 700 W/m^2, (c) 500 W/m^2 and (d) 0 W/m^2 (see online version for colours)

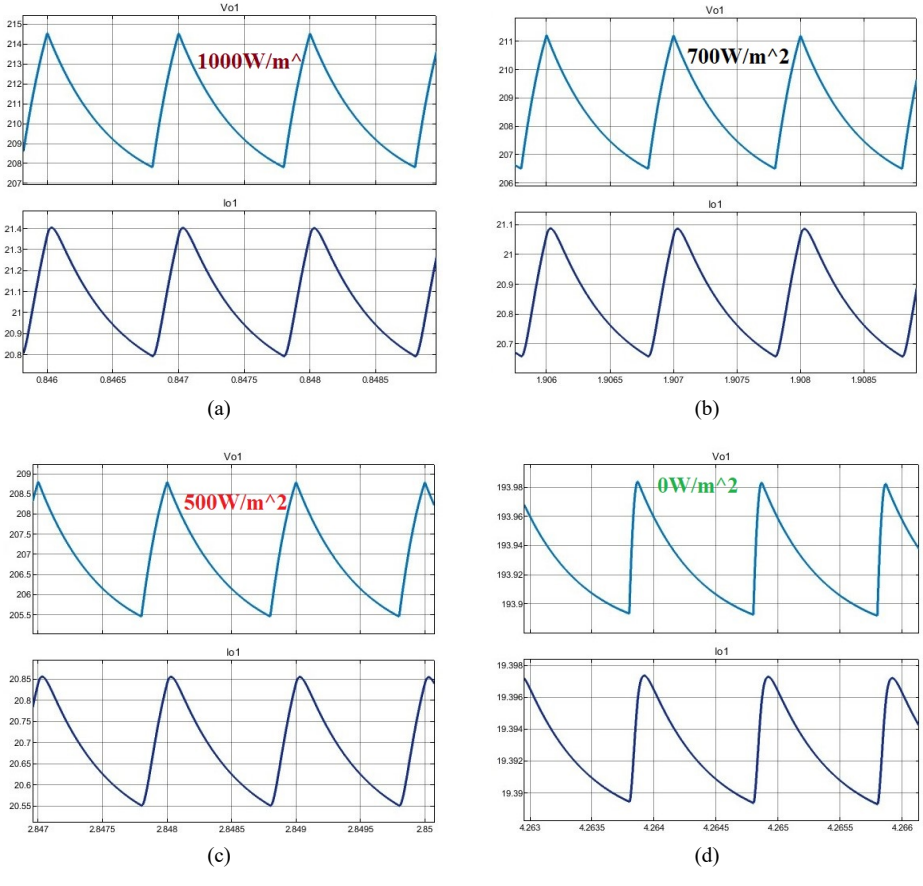

4.2 Device voltages and currents

A single inductor is utilised in the DISO topology. While the irradiance is varied, the magnitude of the average current though the inductor changes. Figure 10 shows the inductor voltage and current waveform with irradiance of 1,000 W/m^2. This value decreases with decreasing irradiance of 700 W/m^2, 500 W/m^2 and 0 W/m^2, respectively. However, the shape of the waveform remains the same thus satisfying the mathematical expression of Kirchoff's voltage balance across the topology.

Figure 13 Charging and discharging of batteries at EV charging station (see online version for colours)

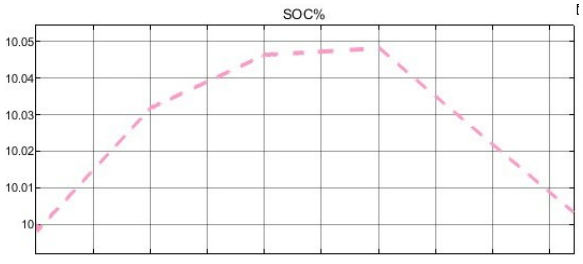

Figure 14 Discharging currents at (a) 1000 W/m^2, (b) 700 W/m^2, (c) 500 W/m^2 and (d) 0 W/m^2 (see online version for colours)

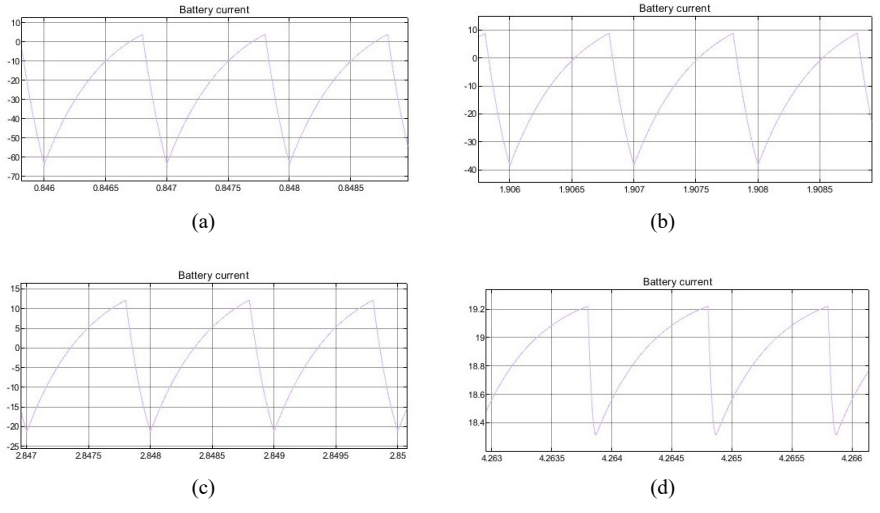

4.2.1 Output voltages and currents

The output voltage and current are DC in nature varying between 200 V to 220 V to support loads at the DC bus of the microgrid. Dropping irradiance affects the voltages but the control strategy maintains the average output voltage at a good approximation of constant level to avoid flickering operation in loads. Figure 11 shows the average

variation in output voltage with varying irradiances at a value of 1,000 W/m^2, 700 W/m^2, 500 W/m^2 and 0 W/m^2, respectively. Figure 12 shows the exact magnitude of the varying voltage levels. It can be observed that even at an irradiance of 0 W/m^2 when the PV source supply is 0 W and the battery is supplying only 36 V, the output DC bus is closely around 200 V.

4.2.2 Vehicle charging and SOC of battery

The charging station is delivering DC power with a constant bus voltage of 200 V. It is observed from Figure 13 that the state of charge (SOC) of batteries in the charging station has a positive slope until the irradiance drops down to 0 W/m^2 when the batteries start discharging and delivering reverse power to the grid.

The negative discharging currents in Figure 14 show charging of battery until 500 W/m^2 irradiance and then discharging at 0 W/m^2 is shown by positive discharging current magnitude. Table 2 shows all the magnitudes of observed currents and voltages across the dual input single output converter.

Table 2 Node voltages and branch currents in the DISO converter

V_{in1}	*72 V (at maximum 1,000 W/m^2)*	$I_{in1(max)}$	*101 A*
V_{in2}	36 V	I_{in2}	100 A
V_0	200 V	I_o	22 A
$V_{L(max)}$	60 V	I_L	220 A
$V_{c(max)}$	200 V	I_c	60 A

5 Control of proposed converter

5.1 Converter voltage gain

From volt second balance in the DISO converter,

$$[V_1 * (D_1T_1) + V_2 * (D_2T_2) = V_o * (D_3T_3)$$

Let,

$$K_1 = (D_2/D_1)$$

and

$$K_2 = (D_3/D_1)$$

Then for converter to work in boost mode,

$$\boxed{V_2/V_1 < 1/(K_2 - K_1)} \tag{8}$$

where $V_2 > V_1$ and for buck operation,

$$\boxed{V_2/V_1 < (K_2 - 1)/(K_1)} \tag{9}$$

where $V_2 > V_1$.

For voltage ranges lying between V_1 and V_2,

$$\boxed{V_2/V_1 > 1/(K_2 - K_1)} \tag{10}$$

In this hybrid mode, converter works as boost for one source and buck for another. Implementing volt second balance when $V_1 = KV_2$ the voltage gain is given by,

$$\boxed{\frac{V_o}{V_{in}} = \left(\frac{D_1K + D_2}{K}\right)} \tag{11}$$

5.2 Control scheme

1-KHz PWM signals generated by the micro-controller Arduino AT-MEGA 2560 are fed to the MOSFET switches in the converter topology. Recurrent sensing and correction yields set reference output at the load end. The PWM generation scheme is shown in Figure 15.

After reviewing contemporary literature for control techniques (Asadi et al., 2023; Shoaei et al., 2023; Lee et al., 2023; Aravind et al., 2024), a control strategy was designed for the proposed DISO as discussed in the previous section. Figure 16 shows the logic implementation for maintaining constant voltage and constant power at the DC bus of the microgrid in case of very low irradiance. Figure 17 shows the implemented bidirectional power flow logic.

There are three cases in such a schematic.

5.2.1 Case 1

When the irradiance is sufficient to provide for the load demand, then battery is disconnected from supply by a switch controlled by ARDUINO MEGA 2560. The DISO considers only PV source and battery is treated as load. In this case, the PV source generates enough power to charge the auxiliary battery source and feed the load.

5.2.2 Case 2

When the irradiance falls lower than the threshold (calculated as 800 W/m^2 in this case), the battery reverses its power flow and acts as an auxiliary power supply. This maintains the voltage profile across load as well as the power demand of the AC and DC microgrids and EV charging station is met. The DISO converter now operates on its full capacity with dual sources at input and a single output at DC bus.

Figure 15 Pulse generation scheme for closed loop control of DISO converter (see online version for colours)

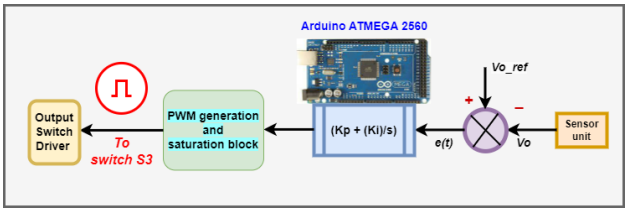

Figure 16 Voltage balancing by PID controller (see online version for colours)

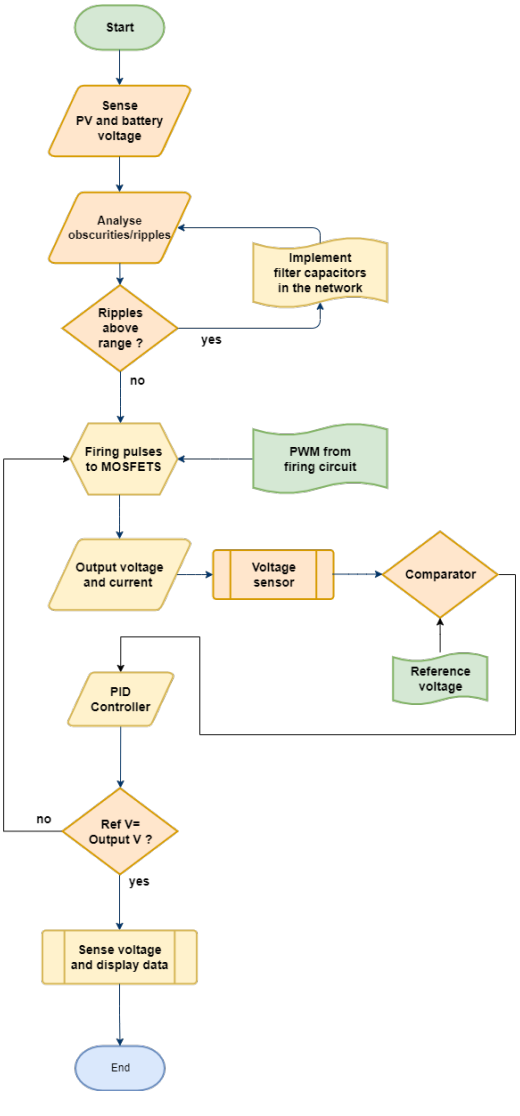

Figure 17 Bidirectional power flow logic by EV charging station (see online version for colours)

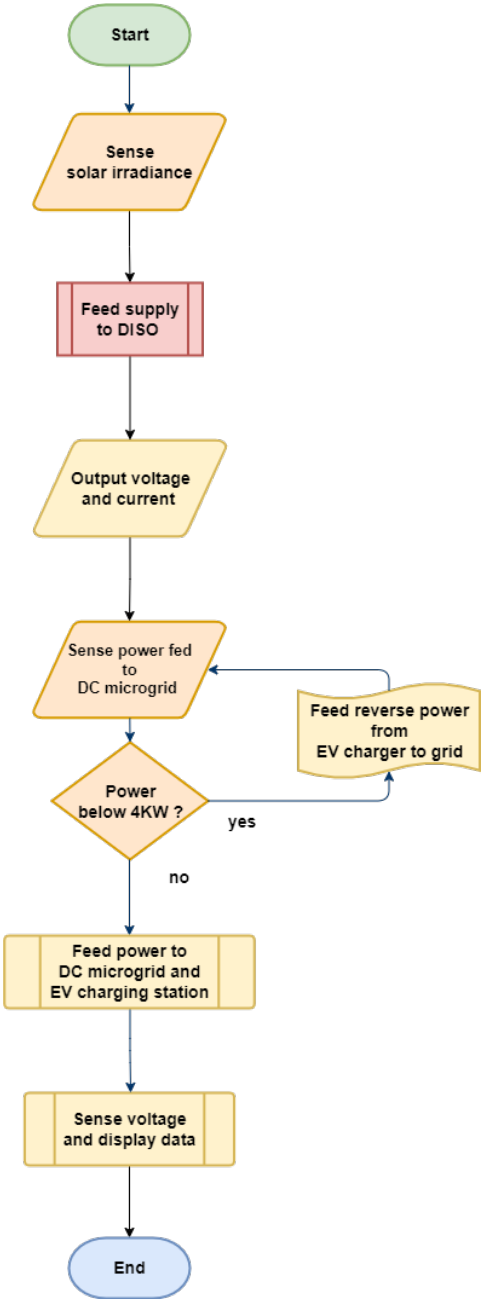

Figure 18 Converter PCB design in (a) 2D, (b) 3D and (c) laboratory prototype (see online version for colours)

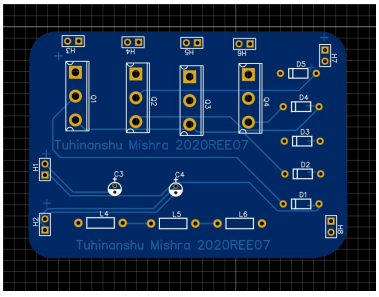

(a)

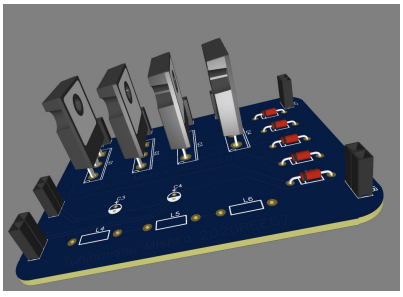

(b)

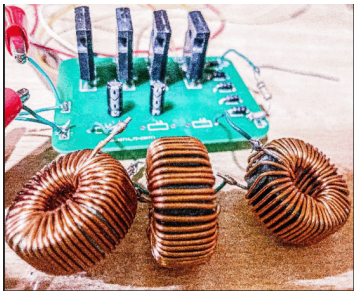

(c)

Figure 19 (a) Laboratory setup and (b) scaled down DSO result for output DC bus voltage (see online version for colours)

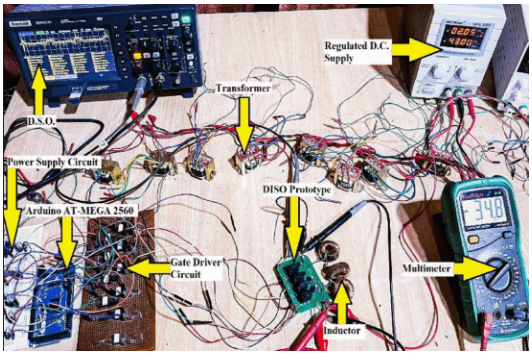

(a)

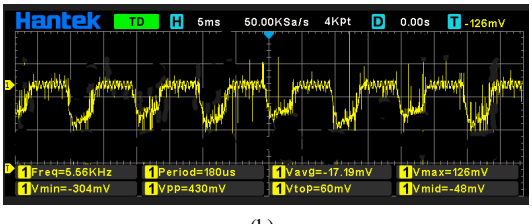

(b)

5.2.3 Case 3

When the irradiance falls much lower, then the EV charger is disconnected from the load and used as a tertiary source of power. In this case also, the power demand is fulfilled. Prioritisation of loads in the order of high to low priority is AC/DC microgrids, auxiliary battery source and EV charging station. The loads are connected and disconnected with this logical priority to meet demand and maintain stability.

Figure 20 DISO converter design on Novacor-RTDS interface RSCAD (see online version for colours)

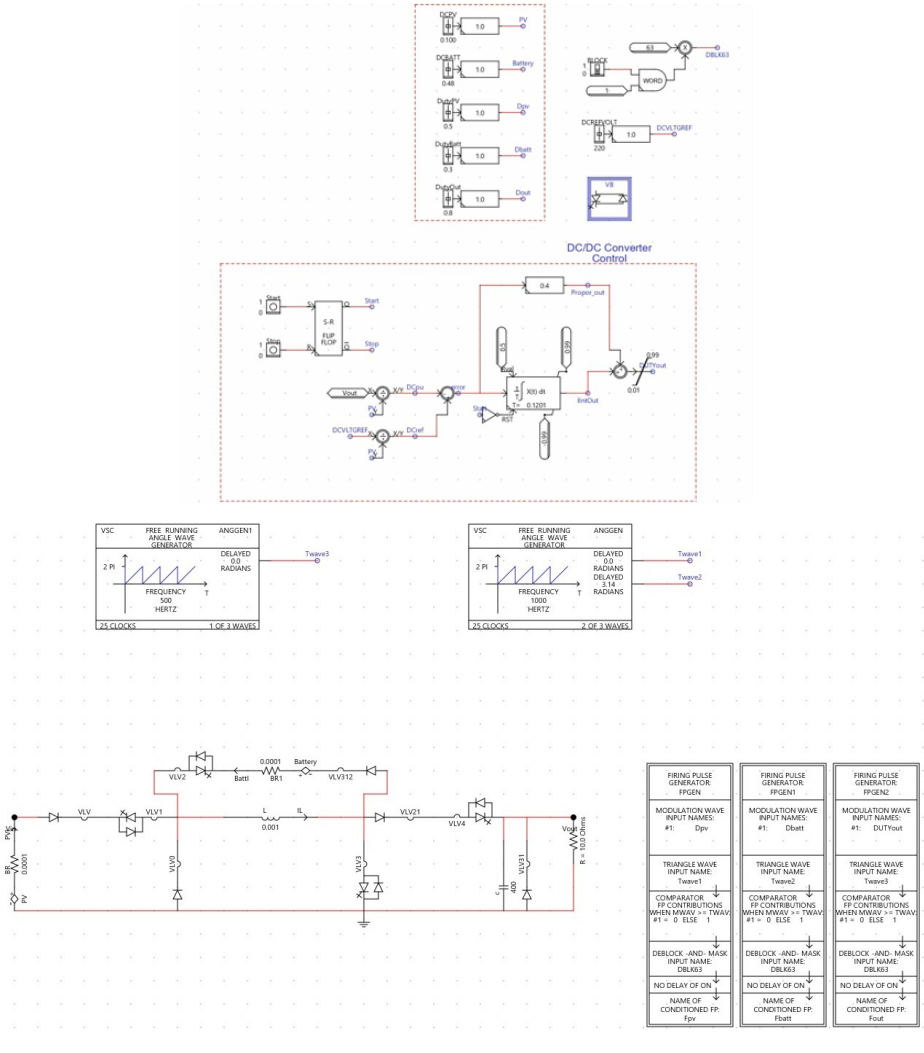

Figure 21 Runtime interface of DISO on RSCAD (see online version for colours)

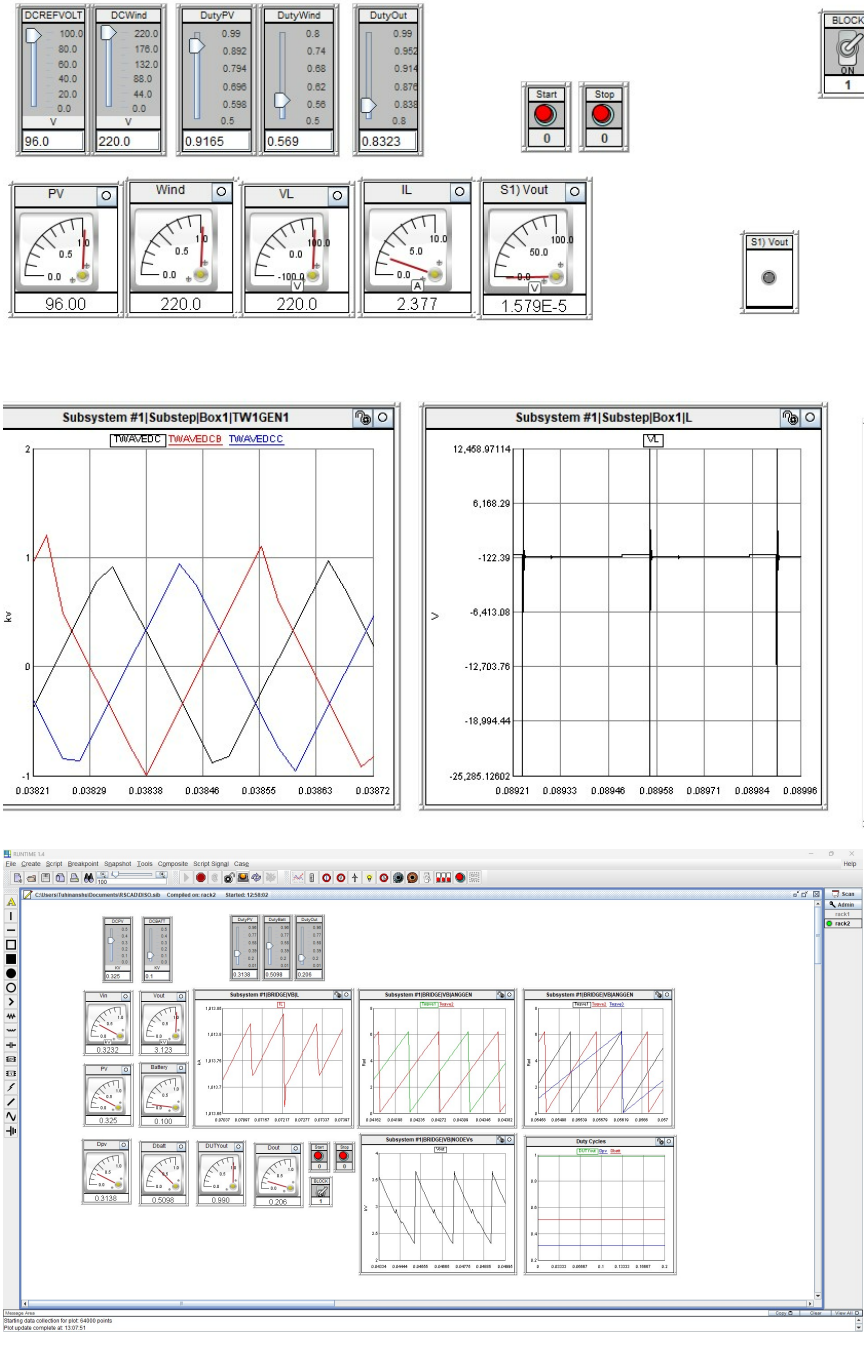

Figure 22 (a) Reference duty cycles, (b) triangular waves and (c) firing pulses (see online version for colours)

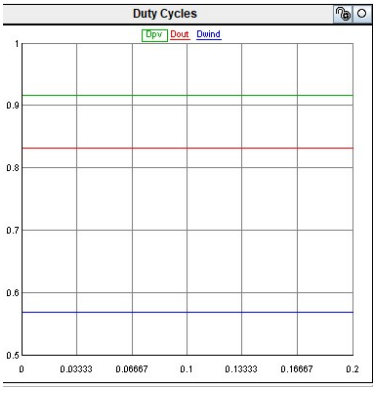

(a)

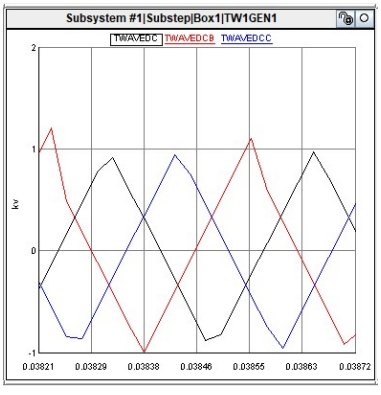

(b)

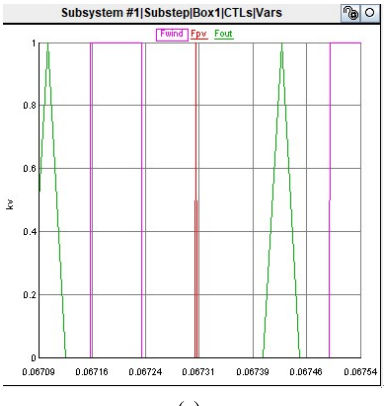

(c)

Figure 23 (a) Inductor current and (b) DC load output voltage (see online version for colours)

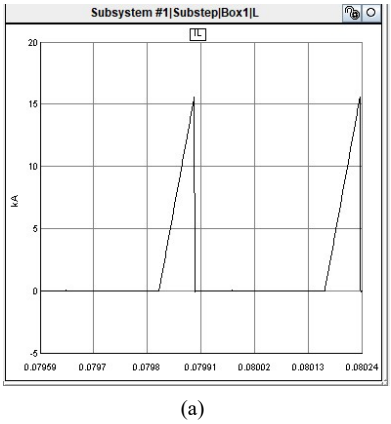

(a)

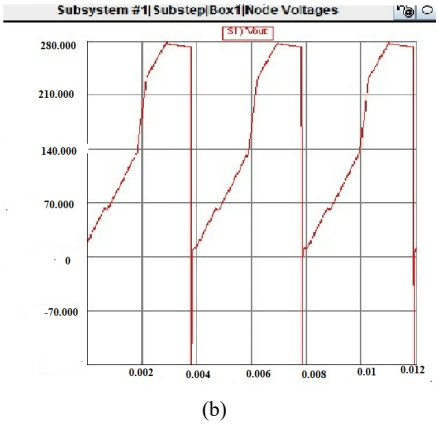

(b)

6 Hardware results and discussion

The converter PCB was designed using Ki-CAD and Easy EDA tools and the prototype was developed. Table 3 shows all component specifications used in the hardware. The converter PCB designs along with a close up of developed DISO is shown in Figure 18 (Mishra and Singh, 2022). The laboratory setup and scaled down result on DSO is shown in Figure 19. A real time simulation of the converter is done on Novacor-RTDS using RSCAD in Figure 20.

Table 3 Hardware component specifications

Component	*Specification*	*Component*	*Specification*
Power MOSFET	IRFP460	Inductor	1 mH ferrite core coil
Bridge rectifier	D2SBA6099	Capacitor	47 microFarad, 470 microFarad
Voltage regulator	L7815CV	Resistor	1 kilo-ohm 5%, 1.7 kilo-ohms 5%, 10 kilo-ohms 5%
Optocouplller	TLP 250	Real time simulator	NOVACOR-RTDS
Power supply	Regulated power supply		
Wires	Solid core jumper wire, Ribbon cable		

The design was done using power electronics library components in RSCAD simulator. A saw-tooth carrier wave was modulated with reference wave to produce required pulses through the firing pulse generators. The switches used in this simulation were IGBT switches with anti-parallel diodes. Figure 21 shows the run-time of DISO simulation on RSCAD. The results obtained for PWM generation in Figure 22 demonstrate that the carrier wave is modulated by three reference duty cycles for DISO converter operating in three modes. The carrier wave is displaced by 120 degrees for equal phase shift. The firing pulse generated as a result are given to each switch. Figure 23 shows inductor current and output voltage waveform.

7 Device analysis and performance parameters

7.1 Stability analysis

The transfer function of the converter is calculated by small signal analysis and is given by,

$$\boxed{\frac{V_o}{V_s} = \frac{RLC^3}{LC(s^3 - D_3^2) + RC^2D_3^2}\begin{bmatrix}\frac{D_3^2D_1}{LC} & \frac{D_3^2D_2}{LC}\end{bmatrix}} \tag{12}$$

where D_1, D_2 and D_3 are duty cycles. The bode plot of transfer function is shown in Figure 24.

The converter is found to be stable for the values of R = 1.5 ohms, L = 1 mH, C = 0.470 mF and the assumed duty cycles.

Figure 24 Magnitude and phase plots for DISO converter (see online version for colours)

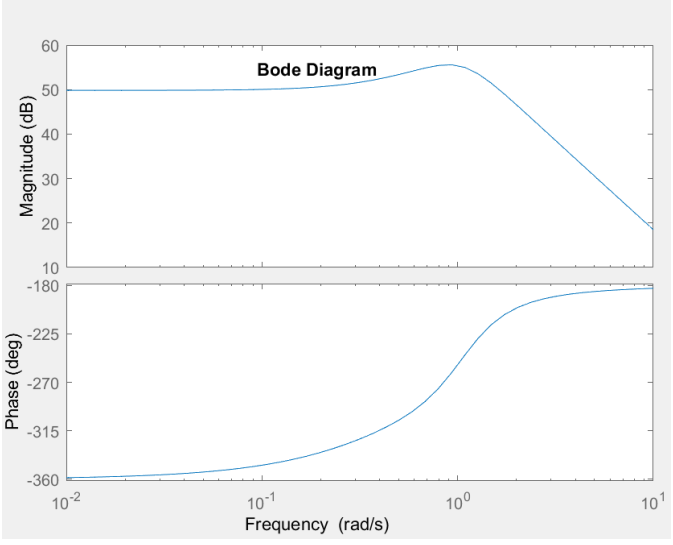

7.2 Loss analysis

The power loss in the converter is the least since the PCB prototype eliminates losses. There are minimum numbers of magnetic components including only single inductor thus further minimising loss. Soft switching of MOSFETs can be done to eliminate any remaining switching loss after the already done minimisation due to the novel PWM scheme.

7.3 Cost analysis

Single inductor and two capacitors are the least possible reactive components that can be used in such a DISO topology thus cost is kept to bare minimum. PCB designing is very prevalent and hence not a very costly process to manufacture the topology in large numbers. Only four switches are used in the topology thus minimising the need of extra firing circuits. The micro-controller used is an Arduino MEGA 2560 which is cheap and easily accessible to everyone. Remaining strain of cost lies on energy supplies. PV panel is in popular demand and distribution of PV panels is increasing rapidly all over the world. Only three lithium-ion batteries are used. It is always a possibility to go for cheaper option and included lead acid batteries.

The converter manufacturing, instalment and use are overall very cheap with minimum maintenance cost required.

7.4 Transients and converter efficiency

The transient response of the proposed topology is shown in Figures 25–26, while Figure 27 shows the efficiency plot with varying time. The steady state efficiency value of the converter on full load is found to be 94.6%.

Figure 25 Transient voltage and current of inductor (see online version for colours)

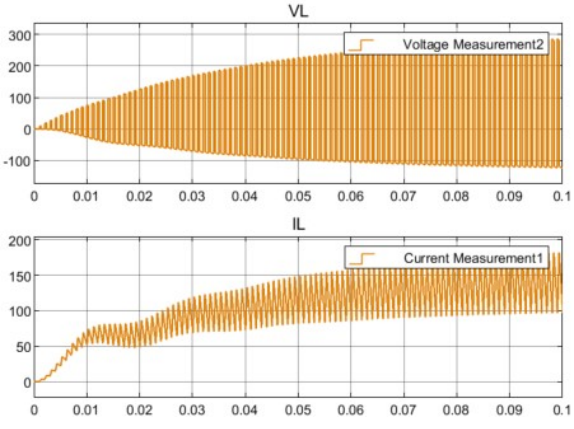

Figure 26 Transient output voltage and current of proposed DISO (see online version for colours)

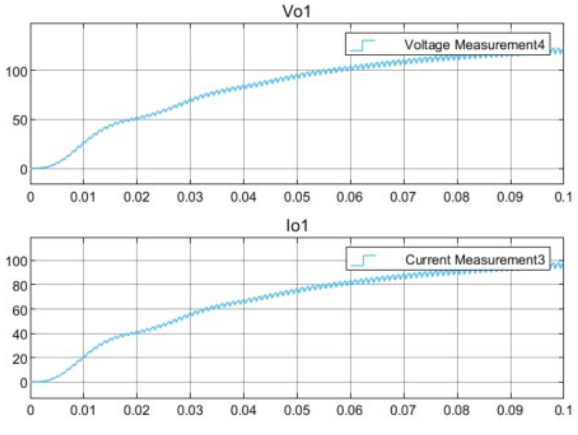

Figure 27 Efficiency of proposed DISO (see online version for colours)

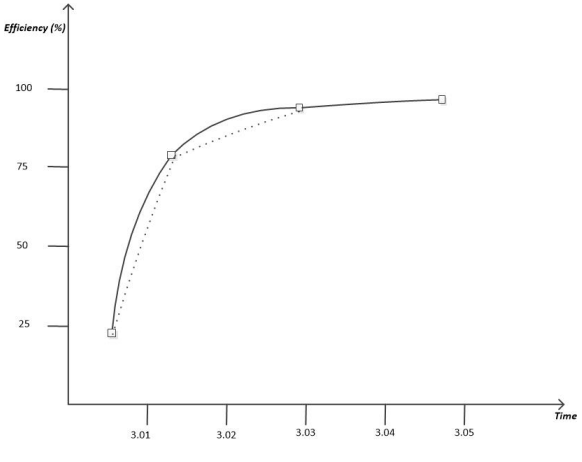

8 Conclusions

The converter thus described was based on a 4-switch novel circuit topology and a 3-pulse novel PWM scheme. The converter was analysed for two cases. A DC microgrid consisting of 4 × 1 KW residential loads and 2-KW EV charging facility was connected at the load end of the DISO converter. An intelligent control algorithm was designed to feed reverse power from EV charging facility to grid along with power from auxiliary battery source if PV irradiance dropped below 700 W/m^2.

When the irradiance drops lower, the PV supplies power supported by the auxiliary source battery which now starts discharging to maintain constant power feed. If the irradiance drops even further, the EV charging facility starts feeding power to the grid thus helping in power balance. The 6-KW load voltage is kept constant at 220 V.

This work introduces a new topology in literature with novelty in PWM as well as its integrated control techniques. The stability analysis along with cost and loss analysis of the converter proves this technology to be of great potential and scope.

References

Akar, F., Tavlasoglu, Y., Ugur, E, Vural, B. and Aksoy, I. (2016) 'A bidirectional non-isolated multi input DC-DC converter for hybrid energy storage systems in electric vehicles', *IEEE Transactions on Vehicular Technology*, Vol. 65, pp.7944–7955, DOI: 10.1109/ TVT.2015.2500683.

Aravind, R., Chokkalingam, B., Verma, R., Aruchamy, S. and Mihet-Popa, L. (2024) 'Multi-port non-isolated DC-DC converters and their control techniques for the applications of renewable energy', *IEEE Access*, Vol. 12, pp.88458–88491, DOI: 10.1109/ ACCESS.2024.3413354.

Asadi, A., Karimzadeh, M.S., Liang, X., Mahdavi, M.S. and Gharehpetian, G.B. (2023) 'A novel control approach for a single-inductor multi-input single-output DC-DC boost converter for PV applications', *IEEE Access*, Vol. 11, pp.114753–114764, DOI: 10.1109/ACCESS. 2023.3324597.

Athikkal, S., Kumar, G.G., Sundaramoorthy, K. and Sankar, A. (2019) 'A non-isolated bridge-type DC-DC converter for hybrid energy source integration', *IEEE Transactions on Industry Applications*, July-August, Vol. 55, No. 4, pp.4033–4043, DOI: 10.1109/TIA. 2019.2914624.

Bussa, V.K., Aman, A. and Singh, R.K. (2021) 'A minimum-phase dual output hybrid converter for standalone hybrid AC/DC supply systems', *IEEE Transactions on Industry Applications*, January–February, Vol. 57, No. 1, pp.1044–1056, DOI: 10.1109/TIA.2020.3035730.

Chen, G., Liu, Y., Qing, X., Ma, M. and Lin, Z. (2021) 'Principle and topology derivation of single-inductor multi-input multi-output DC-DC converters', *IEEE Transactions on Industrial Electronics*, January, Vol. 68, No. 1, pp.25–36.

Dhananjaya, M. and Pattnaik, S. (2020) 'Design and analysis of improved single-input dual-output DC-DC converter', *Electric Power Components and Systems*, June, Vol. 48, Nos. 9–10, pp.906–918, DOI: 10.1080/15325008.2020.1825549.

Kim, H., Maeng, J., Park, I., Jeon, J., Lim, D. and Kim, C. (2021) 'A 90.2% peak efficiency multi-input single-inductor multi-output energy harvesting interface with double-conversion rejection technique and buck-based dual-conversion mode', *IEEE Journal of Solid-State Circuits*, March, Vol. 56, No. 3, pp.961–971, DOI: 10.1109/JSSC.2020.3025722.

Lee, U., Jung, W., Ha, S. and Je, M. (2023) 'An auto-reconfigurable multi-output regulating switched-capacitor DC-DC converter for wireless power reception and distribution in multi-unit implantable devices', *IEEE Open Journal of the Solid-State Circuits Society*, Vol. 3, pp.65–75, 2023, DOI: 10.1109/OJSSCS.2022.3202145.

Malik, M.Z., Farh, H.M.H., Al-Shaalan, A.M., Al-Shamma'a, A.A. and Alhelou, H.H. (2021) 'A novel single-input-multi-output converter for flexible-order power-distributive with MPPT capability', *IEEE Access*, Vol. 9, pp.131020–131032, DOI: 10.1109/ACCESS. 2021.3113729.

Mishra, T. and Singh, R.K. (2022) 'Analysis and hardware implementation of a single inductor dual input single output DC-DC converter for microgrid applications', *2022 International Conference on Power, Energy, Control and Transmission Systems (ICPECTS)*, Chennai, India, pp.1–4, DOI: 10.1109/ICPECTS56089.2022.10047242.

Pires, V.F., Cordeiro, A., Foito, D. and Silva, J.F. (2022) 'A DC-DC converter with capability to support the voltage balance of DC bipolar microgrids', *2022 11th International Conference on Renewable Energy Research and Application (ICRERA*), Istanbul, Turkey, pp.50–55, DOI: 10.1109/ICRERA55966.2022.9922819.

Pires, V.F., Cordeiro, A., Roncero-Clemente, C., Rivera, S. and Dragičević, T. (2023) 'DC-DC converters for bipolar microgrid voltage balancing: a comprehensive review of architectures and topologies', *IEEE Journal of Emerging and Selected Topics in Power Electronics*, February, Vol. 11, No. 1, pp.981–998, DOI: 10.1109/JESTPE.2022.3208689.

Salimi, M., Radmand, F. and Firouz, M.H. (2021) 'Dynamic modeling and closed-loop control of hybrid grid-connected renewable energy system with multi-input multi-output controller', *Journal of Modern Power Systems and Clean Energy*, January, Vol. 9, No. 1, pp.94–103.

Shoaei, A., Abbaszadeh, K. and Allahyari, H. (2023) 'A single-inductor multi-input multilevel high step-up DC-DC converter based on switched-diode-capacitor cells for PV applications', *IEEE Journal of Emerging and Selected Topics in Industrial Electronics*, January, Vol. 4, No. 1, pp.18–27, DOI: 10.1109/JESTIE.2022.3173178.

Sobral, F., Pires, V.F. and Pires, A.J. (2023) 'A DC solid state transformer to interconnect bipolar DC microgrids with voltage balance support', *2023 7th International Young Engineers Forum (YEF-ECE)*, Caparica/Lisbon, Portugal, pp.31–36, DOI: 10.1109/YEF-ECE58420.2023.10209336.

Suresh, K. et al. (2021) 'A multifunctional non-isolated dual input-dual output converter for electric vehicle applications', *IEEE Access*, Vol. 9, pp.64445–64460, DOI: 10.1109/ACCESS.2021.3074581.

Tian, Q., Zhang, X., Zhou, G., Wang, X., Guo, B. and Ma, H. (2023) 'A family of symmetrical bipolar output converters based on voltage-multiplying rectifiers for interfacing renewable energy with bipolar DC microgrid', *IEEE Transactions on Power Electronics*, July, Vol. 38, No. 7, pp.9157–9172, DOI: 10.1109/TPEL.2023.3264257.